Available online at www.CivileJournal.org

Civil Engineering Journal

(E-ISSN: 2476-3055; ISSN: 2676-6957)

Vol. 12, No. 06, June, 2026

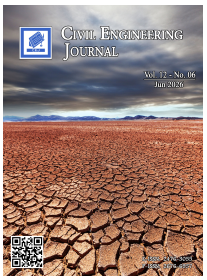

Ambient-Cured Foamed Geopolymer Blocks: Mix Optimization and Microstructural Performance

Prach Amornpinyo [1], Attaphol Bubpi [1], Yongyuth Sirisripetch [1], Tawatchai Tho-In [1], Patcharapol Posi [2*], Phongphan Tankasem [3], Prinya Chindaprasirt [4, 5]

[1] *Department of Civil Technical Education, Faculty of Technical Education, Rajamangala University of Technology Isan, Khon Kaen Campus, Khon Kaen 40000, Thailand.*

[2] *Department of Civil Engineering, Faculty of Engineering, Rajamangala University of Technology Isan, Khon Kaen Campus, Khon Kaen 40000, Thailand.*

[3] *Department of Civil Engineering, Faculty of Engineering, Mahasarakham University, Mahasarakham 44000, Thailand.*

[4] *Sustainable Infrastructure Research and Development Center, Department of Civil Engineering, Faculty of Engineering, Khon Kaen University, Khon Kaen 40002, Thailand.*

[5] *Academy of Science, The Royal Society of Thailand, Bangkok 10210, Thailand.*

Received 16 February 2026; Revised 22 May 2026; Accepted 27 May 2026; Published 01 June 2026

Abstract

This study aims to develop sustainable, ambient-cured lightweight foamed geopolymer blocks utilizing fly ash (FA) and sugarcane bagasse ash (SCBA) to reduce energy consumption in masonry unit production. A comprehensive parametric investigation was conducted on six key mix variables: ordinary Portland cement (OPC) addition, SCBA replacement, foam dosage, liquid-to-binder ratio, alkaline activator ratio, and sand-to-binder ratio. The engineering properties, specifically 7-day compressive strength and bulk density, were evaluated and supported by microstructural characterization using XRD and SEM. The experimental results revealed that the optimum mix comprising a binder of 90% FA and 10% OPC, 10% SCBA replacement, 3% pre-formed foam, a liquid-to-binder ratio of 0.7, a sodium silicate-to-sodium hydroxide ratio of 1.0, and a sand-to-binder ratio of 2.25 was formulated and achieved a lightweight classification (≤ 1,800 kg/m³) with a compressive strength of 9.05 MPa. The significance of this study lies in establishing an optimum mix design that enables the utilization of multiple agro-industrial wastes in structural blocks without the need for energy-intensive thermal curing, thereby offering a viable and eco-friendly alternative for the construction industry.

Keywords: Geopolymer; Lightweight Foamed Geopolymer Block; Fly Ash; Sugarcane Bagasse Ash; Ambient Curing.

1. Introduction

Ordinary Portland cement (OPC) is essential for modern infrastructure, yet its production is a major environmental concern, accounting for approximately 7–8% of global anthropogenic CO_2 emissions [1–3]. This has driven research into alkali-activated materials (AAMs) and geopolymers—aluminosilicate binders derived from industrial or natural precursors—as low-carbon alternatives to conventional concrete. Fundamental studies by Davidovits (1991) & Provis et al. have established the reaction mechanisms and durability of AAMs, particularly those based on fly ash (FA) and metakaolin [4–6]. Among these, Class F fly ash is widely used for geopolymerization due to its availability, although its reactivity under ambient curing depends heavily on particle fineness and chemical composition [7, 8].

* Corresponding author: patcharapol.po@rmuti.ac.th

https://doi.org/10.28991/CEJ-2026-012-06-010

Sugarcane bagasse ash (SCBA), a by-product of the sugar industry, has also emerged as a promising supplementary cementitious material (SCM). When properly ground, SCBA serves as a reactive silica source, improving the strength of cement-based systems and promoting waste valorization [9–11]. Recent work has extended SCBA application to geopolymer systems, showing that it can partially replace FA. However, the performance of these blends is strictly governed by the replacement level and activator chemistry [12, 13]. While sodium hydroxide (NaOH) molarity in the 8–12 M range is generally sufficient for heat-cured systems, higher alkali concentrations (e.g., up to 15 M) are often required under ambient conditions to adequately dissolve less reactive precursors like SCBA and Class F fly ash [12, 14].

Lightweight construction materials are key to decarbonization as they reduce structural dead load and improve thermal insulation. Foamed concretes achieve density reduction (300–1,800 kg/m³) by entraining air bubbles, though this inevitably reduces mechanical strength [15–17]. In geopolymer foam concrete (GFC), achieving a balance between low density and structural integrity is challenging, as porosity, activator modulus, and curing regime all interact to control the final properties [18].

Producing lightweight geopolymer blocks under ambient curing is complicated by the interplay of mix parameters. The sodium silicate-to-sodium hydroxide (NS/NaOH) ratio controls silica availability and setting time; while a ratio near 1.0 often maximizes strength, higher ratios can cause rapid setting or workability issues [19, 20]. Similarly, the liquid-to-binder (L/B) ratio must be optimized to ensure flowability without causing segregation or excessive porosity, with typical optima around 0.6–0.7 [21]. Aggregate packing (sand-to-binder ratio) further influences the internal structure, requiring careful parametric optimization [22].

To enable ambient curing, minor OPC additions (hybrid systems) are often used to accelerate early-age reactions. Studies indicate that 10–30% OPC inclusion can provide sufficient early strength for demolding without heat treatment, keeping the clinker content significantly lower than conventional concrete [23].

Despite the environmental benefits of geopolymers, producing lightweight foamed geopolymer blocks under ambient curing remains a significant challenge. Most previous studies rely heavily on elevated temperature curing to accelerate the polycondensation process and stabilize the pore structure [24, 25]. Under ambient conditions, foamed geopolymers often suffer from slow setting times, foam collapse, and inadequate early-age strength [26]. Furthermore, while SCBA has been utilized as a pozzolanic precursor, its application in ambient-cured foamed systems is rarely reported [27, 28]. To bridge this research gap, this study proposes a hybrid binder system incorporating FA, SCBA, and a minor fraction of OPC. The inclusion of OPC is designed to provide rapid calcium-based reaction products (C-S-H and C-A-S-H gels) to structurally stabilize the pre-formed foam at room temperature, eliminating the need for energy-intensive heat curing while maximizing the utilization of agricultural and industrial wastes.

Therefore, this research aims to (1) quantify the effects of OPC addition (0–15%), SCBA replacement (0–40%), foam dosage (1–4%), L/B ratio (0.5–0.9), NS/NaOH ratio (0.67–1.5), and sand-to-binder ratio (2.00–2.50) on the density and strength of ambient-cured blocks; (2) identify practical mix windows that ensure castability; and (3) propose an optimal mixture satisfying the lightweight density criterion (≤ 1,800 kg/m³) with adequate strength for construction applications.

2. Materials and Methods

2.1. Materials

2.1.1 Binders

The ternary binder system consisted of ordinary Portland cement (OPC), fly ash (FA), and sugarcane bagasse ash (SCBA). Type I OPC, conforming to ASTM C150/C150M-24 [29], was utilized to enhance early-age strength, having a specific gravity of 3.13 and a mean particle size of 14.6 µm. The Class F fly ash, sourced from the Mae Moh power plant in Lampang, Thailand, served as the primary aluminosilicate precursor in accordance with ASTM C618-23 [30] standards (specific gravity: 2.64). The SCBA was obtained from the Eastern Sugar and Cane Public Co., Ltd., Thailand. To enhance its pozzolanic reactivity, the raw ash was ground until it passed through a No. 200 (75-µm) sieve, resulting in a specific gravity of 1.77. As noted in previous studies, this grinding process is critical for increasing the specific surface area and the pozzolanic activity index of the ash [31]. The chemical compositions and physical properties of these binders are summarized in Table 1. The particle size distribution (granulation) curves for all raw materials are illustrated in Figure 1. As observed, the median particle sizes (d50) of OPC, SCBA, and FA are densely grouped at 14.3, 16.5, and 18.7 µm, respectively. This uniform fineness provides a high specific surface area that accelerates alkaline dissolution and ensures a dense binder paste prior to foaming.

Table 1. Chemical composition and physical properties of OPC, FA, and SCBA

Chemical Composition (%)	OPC	FA	SCBA
Silicon dioxide (SiO_2)	21.1	43.1	78.8
Aluminum oxide (Al_2O_3)	4.8	21.9	4.8
Ferric oxide (Fe_2O_3)	3.4	10.8	5.7
Calcium oxide (CaO)	63.4	15.1	4.6
Magnesium oxide (MgO)	2.5	2.7	1.0
Sulfur trioxide (SO_3)	2.3	1.2	0.2
Sodium oxide (Na_2O)	0.2	0.9	0.3
Potassium oxide (K_2O)	0.5	2.5	3.4
Loss on ignition (LOI)	1.8	1.8	1.2
Physical Properties			
Specific Gravity	3.13	2.64	1.77
Median Particle Size (d50, µm)	14.3	18.7	16.5

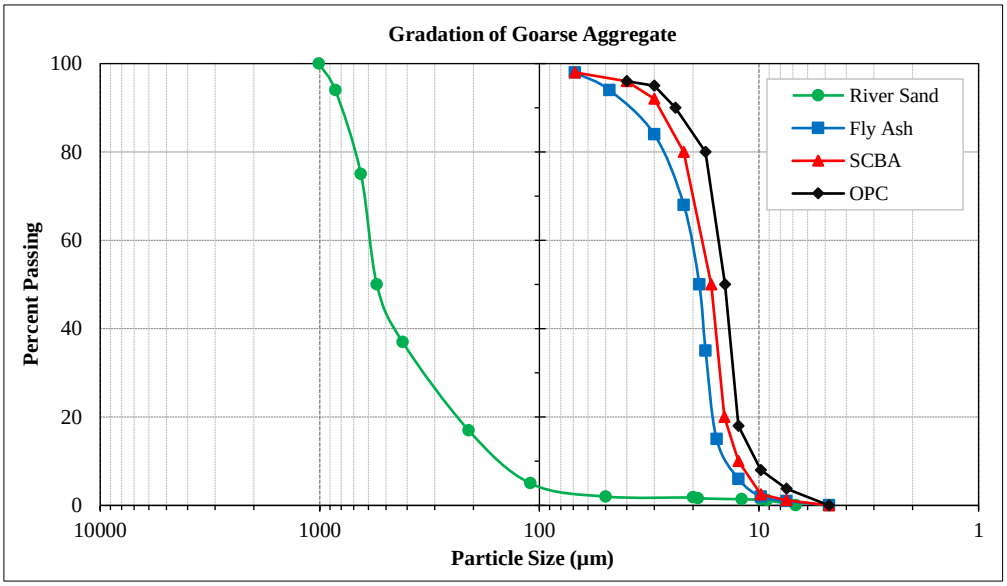

Material	Specification / Preparation	Median Particle Size (d_{50})	Specific Gravity
OPC (Type I)	As received	14.3 µm	3.13
Fly Ash (Class F)	As received	18.7 µm	2.64
SCBA (ground)	Ground and sieved to pass No. 200 (75 µm)	16.5 µm	1.77
River Sand	Sieved to pass No. 16 (1.18 mm)	-	2.57

Note: SCBA was ground and sieved to pass No. 200 sieve (75 µm). River sand was sieved to pass No. 16 sieve (1.18 mm).

Figure 1. Particle size distribution (granulation) curves of the raw materials used in this study

2.1.2. Microstructural and mineralogical characterization of binders

The mineralogical compositions of the binders were investigated using X-ray diffraction (XRD), as illustrated in Figure 2. The diffractogram of Mae Moh fly ash (FA) (Figure 2a) reveals a broad amorphous hump between 20° and 35° (2θ), indicating a substantial content of reactive glassy aluminosilicate phase, which is crucial for geopolymerization. The crystalline phases identified primarily include quartz (SiO_2), mullite ($3Al_2O_3 \cdot 2SiO_2$), hematite (Fe_2O_3), and anhydrite ($CaSO_4$). In contrast, the SCBA pattern (Figure 2b) is dominated by sharp peaks corresponding to quartz, with minor reflections of cristobalite and calcite ($CaCO_3$). A diffuse halo observed in the 15°–25° (2θ) range suggests the presence of amorphous silica derived from the decomposition of sugarcane fibers during combustion [31, 32].

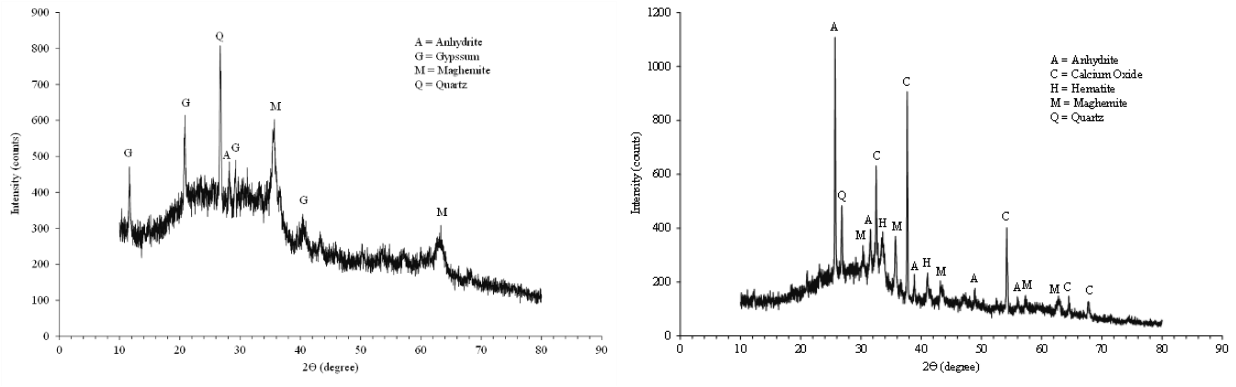

(a) Fly ash (FA) (b) Sugarcane bagasse ash (SCBA)

Figure 2. X-ray diffraction (XRD) patterns of (a) Fly ash (FA) and (b) Sugarcane bagasse ash (SCBA)

Figure 3 presents the morphological characteristics of the binders obtained via scanning electron microscopy (SEM). The FA particles (Figure 3-a) exhibit a predominantly spherical shape with smooth surfaces, characteristic of cenospheres and plerospheres formed during high-temperature suspension firing. This spherical morphology facilitates the "ball-bearing" effect, which enhances the workability and flowability of the fresh geopolymer paste [33]. Conversely, the SCBA particles (Figure 3-b) display irregular, prismatic, and cellular structures with rough textures and high porosity. These morphological features are responsible for the increased water demand and inter-particle friction observed in the SCBA-blended mixtures, necessitating careful adjustment of the liquid content [34].

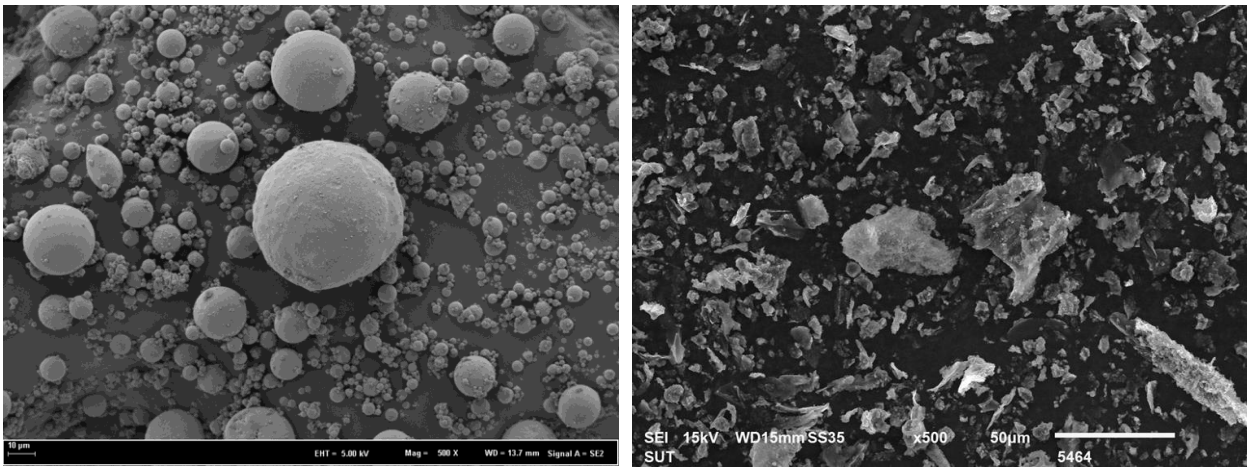

(a) Fly ash particles (b) SCBA particles

Figure 3. Scanning electron microscopy (SEM) images of (a) Fly ash particles and (b) SCBA particles

2.1.3. Aggregates

Locally sourced river sand was used as the fine aggregate. The sand was sieved to pass a No. 16 (1.18 mm) mesh to ensure a uniform texture suitable for thin-joint masonry. Its physical properties included a specific gravity of 2.57, a fineness modulus of 2.75, and a water absorption of 0.85%. The particle size distribution of the prepared river sand, as previously shown in Figure 1, demonstrates a well-graded profile suitable for forming a stable aggregate skeleton within the cellular blocks.

2.1.4 Alkaline Activators and Foam

The alkaline activator was a combination of sodium hydroxide (NaOH) and sodium silicate (Na_2SiO_3) solutions. Commercial-grade NaOH pellets (98% purity) were dissolved in distilled water to prepare a concentration of 15 M. This solution was prepared and allowed to cool to ambient temperature for 24 hours prior to mixing to dissipate reaction heat. For density reduction, a protein-based foaming agent (K-Block Technology Co., Ltd.) was diluted with water at a 1:4 weight ratio. The solution was aerated using a foam generator to produce stable pre-formed foam with a density ranging between 40 and 45 kg/m³ [35]. The overall experimental program and methodology workflow of this study are schematically summarized in Figure 4.

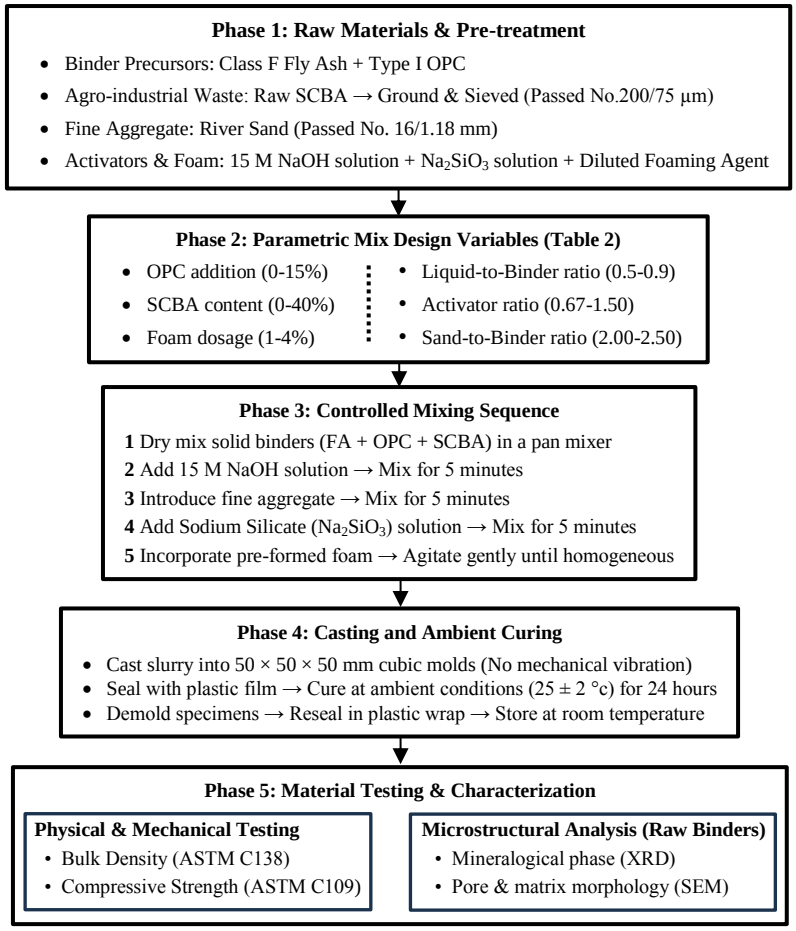

Figure 4. Flowchart of Experimental Methodology

2.2. Mixed Proportions

To systematically optimize the mixture for lightweight applications under ambient curing, a comprehensive parametric study was conducted using a "one-factor-at-a-time" experimental design. This approach allowed for the isolation of individual effects on the physical and mechanical properties of the blocks. As detailed in Table 2, the investigation covered six key mix design variables: (1) OPC replacement level (0–15%), (2) SCBA replacement of the total binder (0–40%), (3) pre-formed foam dosage (1–4%), (4) liquid-to-binder ratio (L/B of 0.5–0.9), (5) alkaline activator ratio (Na_2SiO_3/NaOH of 0.67–1.5), and (6) sand-to-binder ratio (S/B of 2.00–2.50).

Table 2. Summary of mix design parameters and variables investigated

Parameter	Description	Range of Values Investigated
	Binder Composition	
OPC Content	Replacement of FA by weight (%)	0, 5, 10, 15
SCBA Content	Replacement of total binder by weight (%)	0, 10, 20, 30, 40
	Activator & Liquid	
Liquid-to-Binder	L/B ratio (solution/solid binder)	0.5, 0.7, 0.9
Activator Ratio	Sodium Silicate (Na_2SiO_3) to NaOH ratio	0.67 (2:3), 1.0 (3:3), 1.5 (3:2)
	Aggregates & Foam	
Sand-to-Binder	S/B ratio	2.00, 2.25, 2.50
Foam Content	Dosage by weight of total binder (%)	1, 2, 3, 4

The mix proportions were strictly adjusted to achieve the dual objective of maintaining a bulk density ≤ 1,800 kg/m³ while maximizing compressive strength. For all mixtures, the liquid-to-binder ratio (L/B) was defined as the mass ratio of the total alkaline solution (sodium silicate + sodium hydroxide) to the total solid binder content (OPC + FA + SCBA).

2.3. Preparation and Curing

The mixing procedure was carefully designed to ensure matrix homogeneity while preserving the delicate pore structure of the foam. The process began with homogenizing the dry solid binders (FA, OPC, and SCBA) in a pan mixer. To initiate alkaline activation, the 15 M NaOH solution was added to the dry mixture and mixed for 5 minutes. Fine aggregate was then introduced and mixed for an additional 5 minutes to ensure thorough particle coating. Subsequently, the sodium silicate solution (Na_2SiO_3) was added, and mixing continued for another 5 minutes to complete the geopolymeric paste formation. Finally, the pre-formed foam (density 40–45 kg/m³) was incorporated into the slurry. The mixture was gently agitated until the foam was uniformly distributed throughout the matrix.

Immediately after mixing, the fresh paste was cast into 50 × 50 × 50 mm cubic molds. Crucially, the molds were filled and leveled without mechanical vibration to prevent the collapse of the entrained air voids. The specimens were wrapped in plastic film to minimize moisture loss and cured under ambient conditions (25 ± 2 °C). After 24 hours, the samples were demolded, resealed in plastic wrap, and stored at ambient temperature until the testing age. The visual documentation of these experimental procedures and the prepared specimens is presented in Figure 5. This ambient curing regime was selected to simulate practical on-site conditions, relying on the intrinsic self-hardening capacity of the calcium-rich hybrid system [32].

(a) Raw materials

(b) Foam generation and mixing

(c) Casting into 50 mm cubic molds

(d) Wrapping specimens in plastic film for ambient curing

Figure 5. Photographic documentation of the experimental process: (a) raw materials, (b) foam generation and mixing, (c) casting into 50 mm cubic molds, and (d) wrapping specimens in plastic film for ambient curing

2.4. Test Methods

To evaluate the suitability of the developed material as lightweight masonry units, its engineering properties—specifically compressive strength and bulk density—were characterized. Compressive strength testing was performed at an age of 7 days using a Universal Testing Machine (UTM), following the standard protocol of ASTM C109/C109M-21 [36]. To ensure statistical reliability, three cubic specimens were tested for each mix proportion, and the average value was reported. Concurrently, the bulk density was determined by measuring the mass and dimensions of the specimens prior to failure, in accordance with the principles of ASTM C138/C138M-24a [37]. The resulting density values were then benchmarked against the critical threshold of 1,800 kg/m³ to verify compliance with the classification for lightweight concrete blocks.

3. Results and Discussion

Overview: Unless otherwise specified, the reported values represent the mean compressive strength and bulk density obtained from three 50 mm cubic specimens tested at 7 days under ambient curing conditions. The standard deviation is indicated by error bars in the respective figures. The primary criterion for lightweight classification adopted in this study is a bulk density $\rho \leq 1{,}800$ kg/m³. The observed trends are discussed in relation to established literature on foamed concrete and geopolymer systems to contextualize the findings [12, 13, 15–17, 19, 21].

3.1. Effect of OPC-to-FA ratio (0–15%)

The influence of substituting fly ash with OPC (0, 5, 10, and 15 wt%) on the 7-day compressive strength and density of the non-foamed geopolymer mortar is illustrated in Figure 6. The results demonstrate that incorporating minor dosages of OPC significantly enhances the mechanical performance under ambient curing conditions.

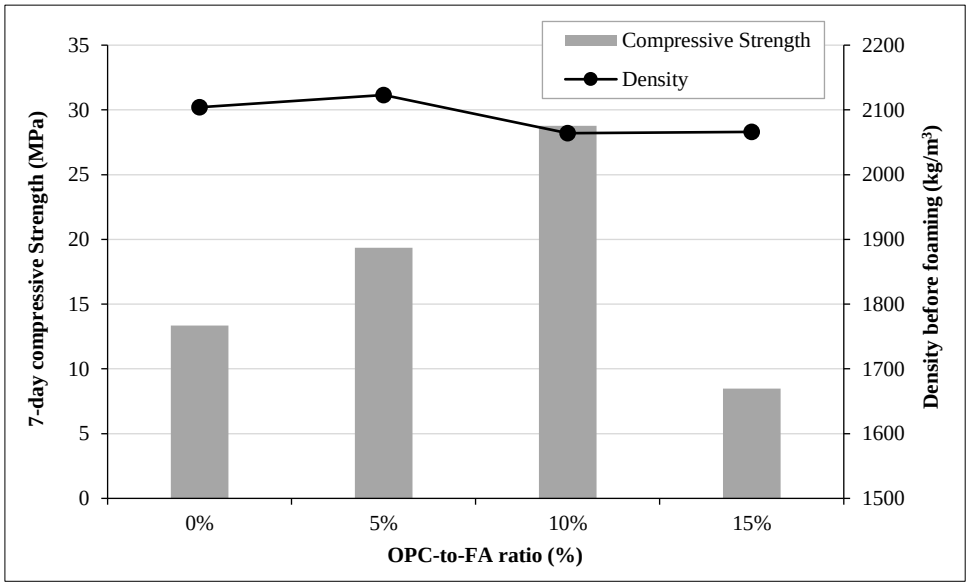

Figure 6. Effect of OPC-to-FA ratio (0, 5, 10, 15%) on 7-day compressive strength and pre-foaming density under ambient curing

As expected, the control formulation (0% OPC) yielded relatively low early-age strength, a characteristic limitation of Class F fly ash geopolymers cured at ambient temperature due to the slow dissolution kinetics of the aluminosilicate glass network [5]. However, the systematic replacement of fly ash with OPC resulted in a marked strength increase, peaking at 28.8 MPa with 10% replacement. This enhancement is attributed to the formation of a hybrid gel system where calcium-rich hydration products, specifically calcium-silicate-hydrate (C-S-H) and calcium-aluminosilicate-hydrate (C-A-S-H) gels, coexist with the primary geopolymeric (N-A-S-H) network. The release of calcium ions (Ca^{2+}) from OPC acts as nucleation seeds, accelerating the hardening process and densifying the microstructure at early ages without requiring thermal activation [5, 23].

Conversely, increasing the OPC content beyond this optimum led to a reduction in compressive strength. This decline is likely associated with the rapid setting behavior induced by excessive calcium availability, which can disrupt the orderly polymerization of the aluminosilicate gel and result in a more heterogeneous or porous microstructure [23]. Regarding physical properties, the variation in density across the series was marginal, with the 10% OPC mix achieving a density of 2,064 kg/m³.

Consequently, an OPC-to-FA ratio of 10% was selected as the optimal baseline for the subsequent foaming experiments. This dosage offers the most favorable balance, maximizing ambient-cured strength while minimizing clinker consumption to align with the study's sustainability objectives. The lightweight specimens exhibited a progressive crushing failure during testing, which is characteristic of cellular concrete. Unlike the brittle, explosive fracture typical of normal-weight high-strength geopolymers, the entrained macro-pores provided a cushioning effect, allowing substantial deformation before ultimate failure. This crushing behavior indicates stable energy absorption suitable for non-load-bearing masonry units.

3.2. Effect of SCBA Replacement (0–40%)

Figure 7 presents the compressive strength evolution when the primary binder (OPC+FA) is partially replaced by SCBA at rates of 0–40%, with the OPC content fixed at 10% of the FA fraction. The results demonstrate a systematic reduction in 7-day compressive strength as the SCBA content increases. The control mix (0% SCBA) achieved the

highest strength at 28.45 MPa. Upon introducing 10% SCBA, the strength decreased to 22.31 MPa and further declined to 14.32 MPa at 40% replacement.

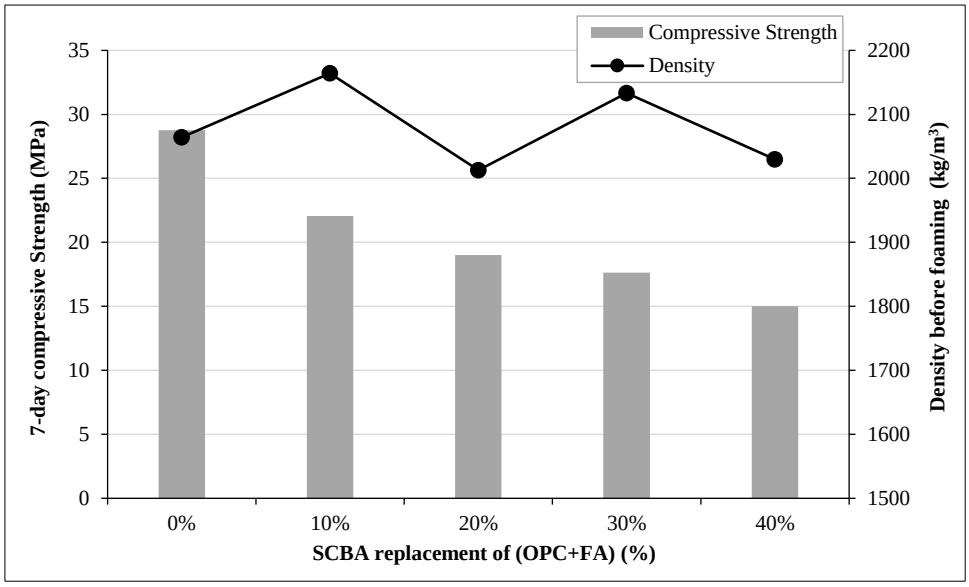

Figure 7. Effect of SCBA replacement of (OPC+FA) at 0–40% on 7-day compressive strength under ambient curing, with other mix parameters held at baseline levels

This downward trend reflects two primary factors. First, the dilution effect: replacing the highly reactive OPC and FA with SCBA reduces the overall availability of dissolved calcium (Ca^{2+}) and aluminosilicate species required for rapid gel formation during the early stages of ambient curing. Second, despite grinding, the SCBA particles typically exhibit a porous morphology and irregular shape compared to the spherical fly ash particles. This characteristic increases the water demand and internal friction, potentially leading to a less compact microstructure and higher porosity [9–13]. It is also worth noting that the unburned carbon in SCBA can physically adsorb the alkaline activator. This absorption reduces the available OH^- and Na^+ ions needed for the initial dissolution of the precursors. As a result, the local alkalinity drops, retarding the early formation of N-A-S-H and C-A-S-H gels and leading to a weaker binder phase.

Implication: Although higher SCBA replacements compromised mechanical performance, the mixture containing 10% SCBA retained a compressive strength exceeding 20 MPa, which is substantial for masonry applications. Therefore, a 10% replacement level was identified as the practical optimum—balancing the ecological benefit of agricultural waste valorization with the necessity of maintaining structural integrity. Unless SCBA reactivity is significantly enhanced through energy-intensive methods (e.g., ultrafine grinding or controlled calcination), low-to-moderate replacement levels are preferable for ambient-cured systems.

3.3. Effect of Foam Content (1–4% by Binder Mass)

The critical trade-off between bulk density and compressive strength as a function of pre-formed foam dosage (1–4 wt%) is illustrated in Figure 8. As anticipated, increasing the foam volume fraction resulted in a systematic reduction in both physical properties due to the introduction of air voids into the geopolymer matrix.

At lower dosages of 1% and 2%, the mixtures failed to meet the lightweight criterion, exhibiting densities of 2,014 kg/m³ and 1,880 kg/m³, respectively. While these mixes maintained relatively high strengths (15.64 MPa and 10.76 MPa), they are classified as normal-weight masonry units.

A pivotal transition occurred at a 3% foam dosage, where the bulk density dropped to 1,747 kg/m³, successfully satisfying the target threshold of ≤ 1,800 kg/m³. Although the compressive strength decreased to 9.22 MPa due to the reduced cross-sectional area and the presence of macro-pores acting as stress concentrators, this value remains sufficient for non-load-bearing applications. Increasing the foam dosage further to 4% resulted in a density of 1,652 kg/m³ but caused a sharp decline in strength to 6.42 MPa, which may compromise structural durability during handling and transportation. The entrained voids inherently act as stress concentrators under compressive loading. As the foam dosage increases, the geopolymer struts (the solid walls separating the air voids) become thinner and more susceptible to buckling and localized microcracking. This microstructural vulnerability explains the sharp, non-linear decline in load-bearing capacity when the foam dosage exceeded 3%.

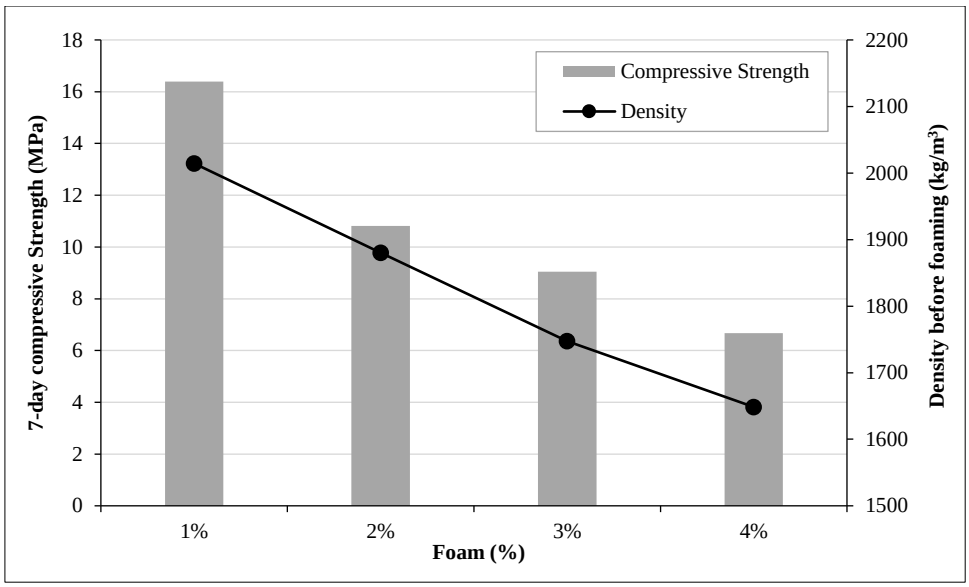

Figure 8. Effect of pre-formed foam dosage on the density–strength trade-off under ambient curing

Implication: Consequently, a 3% foam dosage was established as the optimal baseline. It represents the "tipping point" that achieves the mandatory lightweight classification while retaining the maximum possible mechanical integrity, aligning with established density–strength relationships in cellular concrete literature [15–18].

3.4. Effect of Liquid-to-binder Ratio

Figure 9 illustrates the impact of the liquid-to-binder ratio (L/B = 0.5, 0.7, 0.9) on the 7-day compressive strength and bulk density. The results reveal a clear optimum at an L/B ratio of 0.7.

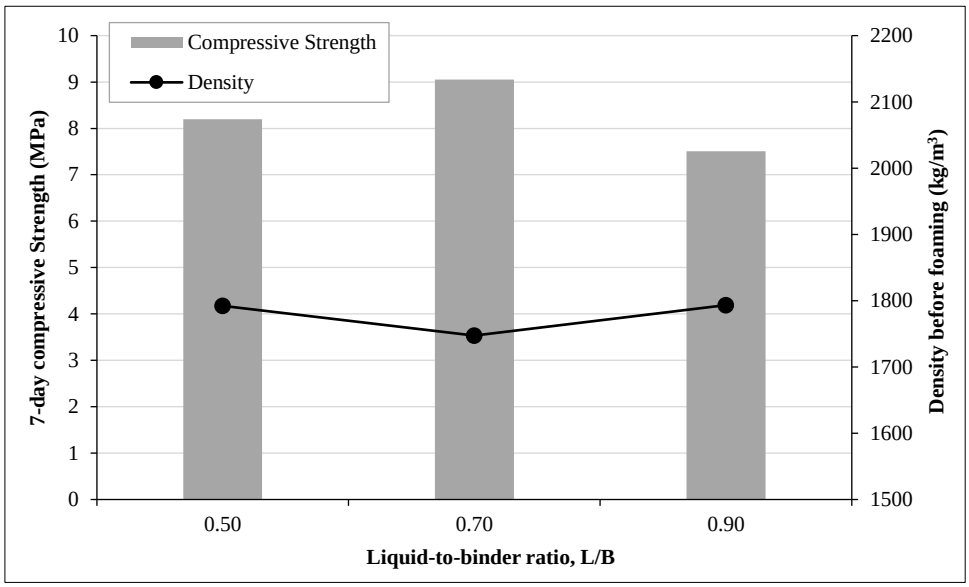

Figure 9. Effect of liquid-to-binder ratio (L/B = 0.5, 0.7, 0.9) on 7-day compressive strength and lightweight compliance ($\rho \leq 1{,}800$ kg/m³) under ambient curing

At a low L/B ratio of 0.5, the mixture exhibited a compressive strength of 8.19 MPa and a density of 1,792 kg/m³. The relatively high density and lower strength can be attributed to the high viscosity of the paste, which hindered the uniform dispersion of the pre-formed foam. This lack of workability has likely caused the foam bubbles to break or coalesce, resulting in a poorly distributed void system.

Increasing the L/B ratio to 0.7 significantly improved the rheology, enabling better mixing and stability. Consequently, the compressive strength peaked at 9.05 MPa, while the density dropped to its lowest value of 1,747 kg/m³. This indicates that an L/B of 0.7 provides the ideal consistency for retaining the entrained air bubbles without segregation, thereby maximizing both lightweight performance and structural integrity.

However, further increasing the L/B ratio to 0.9 resulted in a decrease in strength to 7.51 MPa, with a density of 1,793 kg/m³. The strength reduction in this wet mix is typical of systems with excess liquid, where evaporation leaves behind capillary pores that weaken the matrix. Interestingly, the density increased slightly compared to the 0.7 mix, suggesting that the excess liquid might have caused some foam instability or bubble escape (buoyancy) before setting.

Implication: An L/B ratio of 0.7 is recommended as the optimal parameter, offering the best balance of workability, foam retention (lowest density), and mechanical strength.

3.5. Effect of Activator Ratio (NS/NaOH)

Figure 10 illustrates the influence of the sodium silicate-to-sodium hydroxide mass ratio (NS/NaOH) on the physical and mechanical properties of the ambient-cured blocks. The investigation focused on three critical ratios: 0.67 (2:3), 1.0 (3:3), and 1.5 (3:2).

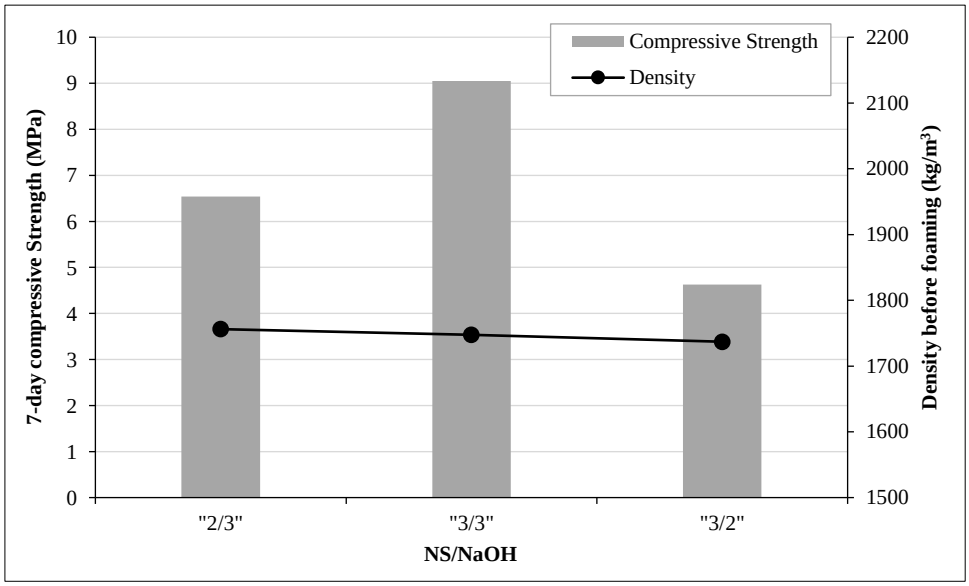

Figure 10. Effect of activator ratio (NS/NaOH = 2/3, 3/3, 3/2) on 7-day compressive strength and lightweight compliance ($\rho \leq 1{,}800$ kg/m³) under ambient curing

The experimental results clearly demonstrate that an NS/NaOH ratio of 1.0 yielded superior mechanical performance, achieving a peak compressive strength of 9.05 MPa with a density of 1,747 kg/m³. This balanced ratio provides an optimal equilibrium between the concentration of soluble silicates (SiO_2)—essential for the condensation of the aluminosilicate gel—and the alkalinity (Na+ and OH-) required to effectively dissolve the fly ash and SCBA precursors [19].

In contrast, reducing the ratio to 0.67 resulted in a significant compromise in strength, which dropped to 6.54 MPa (Density: 1,756 kg/m³). This decline indicates that the lower silicate content restricted the extent of polymerization, leading to a less developed and weaker binder network.

Increasing the ratio further to 1.5 caused a sharp decline in strength to 4.63 MPa (Density: 1,737 kg/m³). This reduction is attributed to the excessive silicate content, which drastically increases the viscosity of the activator solution. High viscosity impairs the workability of fresh paste, making it difficult to achieve uniform compaction. Furthermore, an excess of soluble silicate can induce rapid hardening, which disrupts the orderly reorganization of the geopolymer network, resulting in a heterogeneous and weaker microstructure [20]. An excess of Na_2 SiO_3 introduces a high concentration of soluble Si, which can trigger rapid but incomplete precipitation of silicate oligomers. This premature precipitation often forms a passivating layer around the unreacted fly ash and OPC particles, blocking further alkaline dissolution. Consequently, the system becomes internally "paste-starved" despite the high activator content, leading to the significant strength drop observed at the 1.5 ratio.

Implication: Consequently, an NS/NaOH ratio of 1.0 is identified as the effective activator proportion for this ternary binder system, ensuring the necessary balance for strength development under ambient curing.

3.6. Effect of Sand-to-binder Ratio

Figure 11 illustrates the effect of the sand-to-binder ratio (S/B = 2.00, 2.25, 2.50). The results indicate that the sand content significantly influences the packing density and mechanical properties.

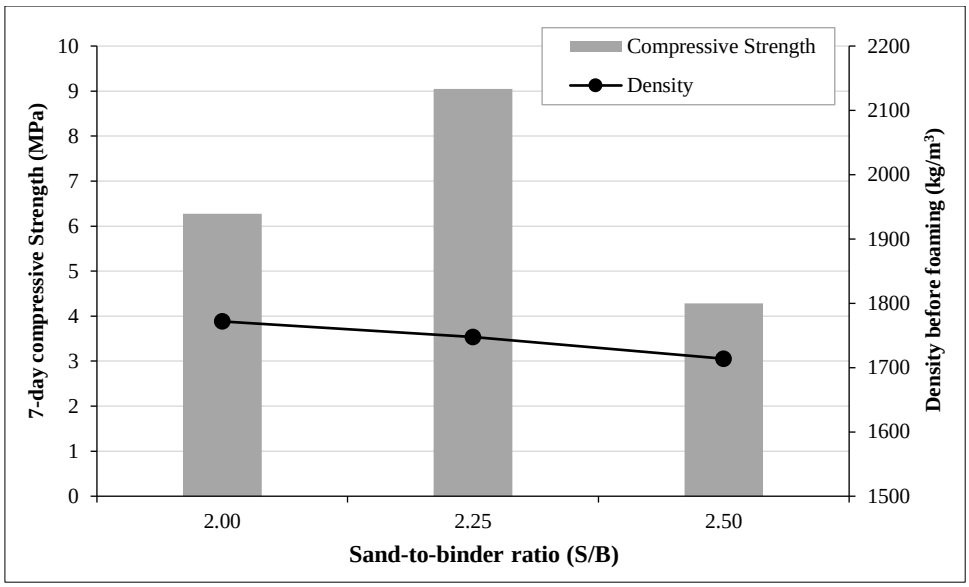

Figure 11. Effect of sand-to-binder ratio (S/B = 2.00, 2.25, 2.50) on 7-day compressive strength and lightweight compliance ($\rho \leq 1{,}800$ kg/m³) under ambient curing

The compressive strength reached its maximum at an S/B ratio of 2.25, with a value of 9.05 MPa and a density of 1,747 kg/m³. At this ratio, the sand particles appear to be optimally packed within the geopolymer paste, providing a robust skeletal framework that resists compressive loads effectively.

When the S/B ratio was lower (2.00), the strength dropped to 6.27 MPa (Density: 1,772 kg/m³). This may be attributed to the lower volume fraction of the rigid aggregate phase, making the composite more susceptible to shrinkage-induced microcracking.

Conversely, increasing the S/B ratio to 2.50 resulted in the lowest strength of 4.28 MPa (Density: 1,714 kg/m³). Although this mix was the lightest, the sharp decline in strength indicates a "paste-starved" condition. With insufficient binder to fully coat the high surface area of the aggregates, the Interfacial Transition Zone (ITZ) becomes weak and porous, compromising the overall load-bearing capacity [22].

Implication: Consequently, an S/B ratio of 2.25 was selected as the optimum, balancing aggregate interlocking with sufficient binder coverage.

3.7. Integrated Optimum Window and Mix Design Guidance

Synthesizing the results from the parametric investigation, we have identified a specific "optimum mix window" for producing ambient-cured lightweight geopolymer blocks. The ideal formulation consists of:

- Binder: 90% Fly Ash + 10% OPC (to ensure ambient curing);
- SCBA Replacement: 10% of the total binder (to balance waste utilization and strength);
- Foam Dosage: 3% by weight (to achieve density $\leq 1{,}800$ kg/m³);
- Activator: NS/NaOH ratio of 1.0 with an L/B ratio of 0.7;
- Aggregate: Sand-to-binder ratio (S/B) of 2.25.

Within this window, the mixtures successfully meet the lightweight criterion ($\rho \leq 1{,}800$ kg/m³) while delivering sufficient compressive strength for non-load-bearing masonry applications. This performance relies on a synergy of mechanisms: the minor OPC addition promotes early calcium-based gel formation; the pre-formed foam tailors the pore structure; the intermediate L/B ratio balances dissolution limits against porosity; the NS/NaOH ratio of 1.0 supplies reactive silica without inducing flash set; and the optimal S/B ratio ensures effective load transfer through the aggregate skeleton [5, 15, 19, 21].

Implication: The S/B ratio of 2.25 is highlighted as the critical parameter for physical stability, offering the best balance between particle packing and the availability of binder paste for gel bridging.

When placed in the context of recent literature on cellular geopolymers, the optimized mix shows highly competitive results. Many previous studies on lightweight fly ash geopolymers have relied on elevated temperature curing to reach acceptable early-age strengths within the 1,600–1,800 kg/m³ density range. However, by introducing 10% OPC and 10% SCBA as a hybrid binder, a 7-day compressive strength of 9.05 MPa was achieved under ambient curing (25 °C). This approach bypasses the energy-intensive heat curing usually needed for Class F fly ash activation [27]. Moreover, while most research has focused primarily on industrial by-products, successfully integrating an agricultural residue like

SCBA without failing the lightweight masonry criteria demonstrates a much more practical and sustainable route for large-scale block manufacturing.

3.8. Practical Considerations and Limitations

Castability and Production Constraints: The experimental trials highlighted the sensitivity of the mix to activator chemistry. Specifically, increasing the NS/NaOH ratio toward 1.5 resulted in highly viscous pastes that were difficult to cast and level without vibration. For plant-scale production, strict control of the silicate modulus is essential to maintain consistent rheology and foam stability. The NS/NaOH ratio near 1.0 is recommended to ensure ease of placement and to prevent rapid setting issues [19, 20].

SCBA Variability: The performance of the blocks is inherently linked to the quality of the agricultural by-product. Since SCBA properties can vary significantly based on combustion conditions, the recommended 10% replacement level serves as a conservative baseline. If higher replacement levels are desired for greater sustainability, the SCBA may require optimized calcination or finer grinding to enhance its pozzolanic reactivity [9, 11].

High Alkalinity Requirement: While the proposed mix successfully eliminates the need for thermal curing, it relies on a high activator concentration (15 M NaOH) to compensate for the slow room-temperature reactivity of the fly ash and SCBA. The use of such a high molarity introduces significant cost and safety challenges. Since 15 M NaOH is highly corrosive, the large-scale production of these blocks cannot be performed via conventional on-site mixing. Instead, manufacturing must be strictly confined to controlled precast facilities equipped with automated mixing systems and proper safety protocols. Future research should focus on optimizing the precursors, perhaps through finer grinding, to lower the required NaOH concentration and improve overall cost-efficiency.

Microstructural Characterization Limitations: While the current SEM and XRD analyses provide solid qualitative insights into the binder morphology and gel formation, the use of quantitative pore analysis such as porosity measurement or image analysis of pore distribution would be instrumental for the full picture analyses of the study.

Sustainability Trade-off: Incorporating 10% OPC slightly increases the carbon footprint of the binder compared to a full alkali-activated system. However, this negative impact is heavily offset by the elimination of thermal curing. Conventional fly ash geopolymers require substantial energy for temperature curing, whereas this hybrid system hardens at room temperature. Consequently, the overall energy demand and net CO_2 emissions are minimized, maintaining a clear long-term sustainability advantage over traditional cement blocks.

Durability and Long-term Performance: While this study establishes the feasibility of 7-day performance under ambient curing, real-world application requires long-term validation. Future work should extend the monitoring period to 28 and 56 days and include durability assessments—such as water absorption, thermal conductivity, and resistance to acid/sulfate attack—to fully qualify these materials for diverse construction environments [17, 18]. It should be noted that longer curing periods (28 or 56 days) will further increase the compressive strength due to ongoing pozzolanic reactions. Meanwhile, the bulk density will slightly decrease as free moisture evaporates, which only further secures the lightweight classification of the blocks.

4. Conclusion

This study successfully demonstrated the feasibility of producing ambient-cured lightweight geopolymer blocks by integrating Class F fly ash with ordinary Portland cement (OPC) and sugarcane bagasse ash (SCBA). A major challenge in conventional fly ash geopolymers is the necessity for heat activation. However, substituting 10% of the fly ash with OPC provided essential calcium species, triggering the formation of a hybrid C-A-S-H and N-A-S-H gel network that allowed the system to harden efficiently at a room temperature of 25 °C. Furthermore, incorporating 10% SCBA served as a practical pathway to valorize agricultural waste. While higher SCBA contents reduced the early-age compressive strength—primarily due to unburned carbon absorbing the alkaline activator and lowering the local pH—the 10% replacement level maintained structural integrity. To meet the lightweight masonry criteria, pre-formed foam was introduced. The experimental results revealed that a 3% foam dosage (by binder weight) was the critical threshold. It effectively lowered the bulk density to below 1,800 kg/m³ without causing a severe collapse in the load-bearing capacity, although the entrained macro-pores inherently acted as stress concentrators that shifted the failure mode to a progressive crushing behavior.

Through systematic parametric evaluation, the physical and mechanical properties proved to be highly sensitive to the activator chemistry and mixture proportions. An optimal liquid-to-binder (L/B) ratio of 0.7 and a sodium silicate-to-sodium hydroxide (NS/NaOH) ratio of 1.0 provided the ideal workability and soluble silica concentration, preventing premature setting while ensuring uniform foam dispersion. Additionally, a sand-to-binder ratio of 2.25 yielded the best aggregate packing density. Combining these optimal parameters, the finalized lightweight block achieved a 7-day compressive strength of 9.05 MPa and a density of 1,747 kg/m³ entirely under ambient curing. Ultimately, this research highlights an energy-efficient approach to manufacturing sustainable construction materials. By removing the dependency on thermal curing and successfully incorporating both industrial and agricultural by-products, the proposed ternary geopolymer system offers a viable, low-carbon alternative to conventional cement-based lightweight masonry units.

5. Declarations

5.1. Author Contributions

Conceptualization, P.A., P.P., and P.C.; methodology, P.A., A.B., T.T., and P.T.; validation, Y.S., P.P., and P.C.; formal analysis, P.A. and P.P.; investigation, P.A., A.B., T.T., P.T., Y.S., and P.P.; resources, P.A., P.C., and P.P.; data curation, P.A., A.B., Y.S., and P.P.; writing—original draft preparation, P.A.; writing—review and editing, P.P. and P.C.; visualization, P.A., A.B., T.T., P.T., Y.S., and P.P.; supervision, P.C. and P.P.; project administration, P.A. All authors have read and agreed to the published version of the manuscript.

5.2. Data Availability Statement

The data presented in this study are available on request from the corresponding author.

5.3. Funding and Acknowledgments

This research was supported by the Rajamangala University of Technology Isan (Khon Kaen Campus). The last author would like to acknowledge the “Support by Research and Graduate Studies” Khon Kaen University.

5.4. Conflicts of Interest

The authors declare no conflict of interest.

6. References

[1] Andrew, R. M. (2018). Global CO2 emissions from cement production. Earth System Science Data, 10(1), 195–217. doi:10.5194/essd-10-195-2018.

[2] Barbhuiya, S., Kanavaris, F., Das, B. B., & Idrees, M. (2024). Decarbonising cement and concrete production: Strategies, challenges and pathways for sustainable development. Journal of Building Engineering, 86, 108861. doi:10.1016/j.jobe.2024.108861.

[3] Volaity, S. S., Aylas-Paredes, B. K., Han, T., Huang, J., Sridhar, S., Sant, G., Kumar, A., & Neithalath, N. (2025). Towards decarbonization of cement industry: a critical review of electrification technologies for sustainable cement production. NPJ Materials Sustainability, 3(1), 23. doi:10.1038/s44296-025-00068-6.

[4] Davidovits, J. (1991). Geopolymers - Inorganic polymeric new materials. Journal of Thermal Analysis, 37(8), 1633–1656. doi:10.1007/BF01912193.

[5] Provis, J. L., & Bernal, S. A. (2014). Geopolymers and related alkali-activated materials. Annual Review of Materials Research, 44, 299–327. doi:10.1146/annurev-matsci-070813-113515.

[6] Provis, J. L. (2018). Alkali-activated materials. Cement and Concrete Research, 114, 40–48. doi:10.1016/j.cemconres.2017.02.009.

[7] Castillo, H., Collado, H., Droguett, T., Sánchez, S., Vesely, M., Garrido, P., & Palma, S. (2021). Factors affecting the compressive strength of geopolymers: A review. Minerals, 11(12), 1317. doi:10.3390/min11121317.

[8] Ahmed, H. U., Mohammed, A. A., Rafiq, S., Mohammed, A. S., Mosavi, A., Sor, N. H., & Qaidi, S. M. (2021). Compressive strength of sustainable geopolymer concrete composites: a state-of-the-art review. Sustainability, 13(24), 13502. doi:10.3390/su132413502.

[9] Cordeiro, G. C., Toledo Filho, R. D., Tavares, L. M., & Fairbairn, E. M. R. (2008). Pozzolanic activity and filler effect of sugar cane bagasse ash in Portland cement and lime mortars. Cement and Concrete Composites, 30(5), 410–418. doi:10.1016/j.cemconcomp.2008.01.001.

[10] Maldonado-García, M. A., Hernández-Toledo, U. I., Montes-García, P., & Valdez-Tamez, P. L. (2018). The influence of untreated sugarcane bagasse ash on the microstructural and mechanical properties of mortars. Materiales de Construccion, 68(329), 148. doi:10.3989/mc.2018.13716.

[11] Thomas, B. S., Yang, J., Bahurudeen, A., Abdalla, J. A., Hawileh, R. A., Hamada, H. M., Nazar, S., Jittin, V., & Ashish, D. K. (2021). Sugarcane bagasse ash as supplementary cementitious material in concrete – a review. Materials Today Sustainability, 15, 100086. doi:10.1016/j.mtsust.2021.100086.

[12] Rihan, M. A. M., Alahmari, T. S., Onchiri, R. O., Gathimba, N., & Sabuni, B. (2024). Impact of Alkaline Concentration on the Mechanical Properties of Geopolymer Concrete Made up of Fly Ash and Sugarcane Bagasse Ash. Sustainability (Switzerland), 16(7), 2841. doi:10.3390/su16072841.

[13] Muradyan, N., Arzumanyan, A., Kalantaryan, M., Khachatryan, K., Zendri, E., & Arzumanyan, A. (2025). Geopolymer Mortars from Tuff Waste: A Circular Approach. Civil Engineering Journal, 11(10), 4092–4107. doi:10.28991/CEJ-2025-011-10-07.

[14] Wardhono, A. (2018). The Effect of Sodium Hydroxide Molarity on Strength Development of Non-Cement Class C Fly Ash Geopolymer Mortar. Journal of Physics: Conference Series, 947(1), 12001. doi:10.1088/1742-6596/947/1/012001.

[15] Ramamurthy, K., Kunhanandan Nambiar, E. K., & Indu Siva Ranjani, G. (2009). A classification of studies on properties of foam concrete. Cement and Concrete Composites, 31(6), 388–396. doi:10.1016/j.cemconcomp.2009.04.006.

[16] Othman, R., Jaya, R. P., Muthusamy, K., Sulaiman, M., Duraisamy, Y., Abdullah, M. M. A. B., Przybył, A., Sochacki, W., Skrzypczak, T., Vizureanu, P., & Sandu, A. V. (2021). Relation between density and compressive strength of foamed concrete. Materials, 14(11), 2967. doi:10.3390/ma14112967.

[17] Amran, M., Fediuk, R., Vatin, N., Lee, Y. H., Murali, G., Ozbakkaloglu, T., Klyuev, S., & Alabduljabber, H. (2020). Fibre-reinforced foamed concretes: A review. Materials, 13(19), 1–36. doi:10.3390/ma13194323.

[18] Rashad, A. M., Mosleh, Y. A., & Mokhtar, M. M. (2024). Thermal insulation and durability of alkali-activated lightweight slag mortar modified with silica fume and fly ash. Construction and Building Materials, 411, 134255. doi:10.1016/j.conbuildmat.2023.134255.

[19] Morsy, M. S., Alsayed, S. H., Al-Salloum, Y., & Almusallam, T. (2014). Effect of Sodium Silicate to Sodium Hydroxide Ratios on Strength and Microstructure of Fly Ash Geopolymer Binder. Arabian Journal for Science and Engineering, 39(6), 4333–4339. doi:10.1007/s13369-014-1093-8.

[20] Wardhono, A., Risdianto, Y., Sabariman, B., Hidajati, N. W., & Andajani, N. (2023). The Effect of Sodium Silicate to NaOH Ratio on Strength Development of Fly Ash Geopolymer Mortar in Marine Environment. E3S Web of Conferences, 445, 1005. doi:10.1051/e3sconf/202344501005.

[21] Verma, M., & Dev, N. (2022). Effect of Liquid to Binder Ratio and Curing Temperature on the Engineering Properties of the Geopolymer Concrete. Silicon, 14(4), 1743–1757. doi:10.1007/s12633-021-00985-w.

[22] Naghizadeh, A., & Ekolu, S. O. (2018). Effect of mix parameters on strength of geopolymer mortars-experimental study. 6th International Conference on Durability of Concrete Structures, ICDCS 2018, 18-20 July, 2018, Leeds, United Kingdom.

[23] Rojas-Duque, O., Espinosa, L. M., Robayo-Salazar, R. A., & de Gutiérrez, R. M. (2020). Alkali-activated hybrid concrete based on fly ash and its application in the production of high-class structural blocks. Crystals, 10(10), 946. doi:10.3390/cryst10100946.

[24] Nguyễn, P. H., Nguyễn, H. H., Lương, Q.-H., Kim, Y., & Lee, B. Y. (2026). Ambient Temperature Curing Stimulated One-Part Engineered Geopolymer Composites with Extremely High Ductility and Low Thermal Conductivity. Journal of Materials in Civil Engineering, 38(4). doi:10.1061/jmcee7.mteng-22099.

[25] Le, D. H., Phan, V. T. A., & Vo, V. T. (2026). Fly ash–sugarcane bagasse ash geopolymer materials: curing optimization and evaluation of strength, shrinkage, and sulfate resistance. Innovative Infrastructure Solutions, 11(5), 261. doi:10.1007/s41062-026-02667-1.

[26] Vo, V. T., Le, D. H., & Phan, V. T. A. (2026). Optimisation of alkaline solution for fly ash-sugarcane bagasse ash geopolymer mortars: effects on strength, durability, and microstructure. European Journal of Environmental and Civil Engineering, 30(1), 2604297. doi:10.1080/19648189.2025.2604297.

[27] Lương, Q. H., Nguyễn, H. H., Nguyễn, P. H., Park, S. E., Kim, Y., & Lee, B. Y. (2025). Achieving ultra-ductility exceeding 13 % and cost efficiency with rubberized alkali-activated slag-based cement-free composites. Developments in the Built Environment, 22, 100677. doi:10.1016/j.dibe.2025.100677.

[28] Pratap, B., Kumar, S., Gupta, K. K., Reddy, N. G., Rashid, A., Asaithambi, P., & Karuppannan, S. (2026). Mechanical properties analysis of geopolymer concrete based on the sugarcane bagasse ash using machine learning. Scientific Reports, 16(1), 14485. doi:10.1038/s41598-026-44848-z.

[29] ASTM C150/C150M-24. (2021). Standard Specification for Portland Cement. ASTM International, Pennsylvania, United States. doi:10.1520/C0150_C0150M-24.

[30] ASTM C618-23. (2010). Standard Specification for Coal Ash and Raw or Calcined Natural Pozzolan for Use in Concrete. ASTM International, Pennsylvania, United States. doi:10.1520/C0618-23.

[31] Cordeiro, G. C., Toledo Filho, R. D., Tavares, L. M., & Fairbairn, E. de M. R. (2009). Ultrafine grinding of sugar cane bagasse ash for application as pozzolanic admixture in concrete. Cement and Concrete Research, 39(2), 110–115. doi:10.1016/j.cemconres.2008.11.005.

[32] Somna, K., Jaturapitakkul, C., Kajitvichyanukul, P., & Chindaprasirt, P. (2011). NaOH-activated ground fly ash geopolymer cured at ambient temperature. Fuel, 90(6), 2118–2124. doi:10.1016/j.fuel.2011.01.018.

[33] Wongkvanklom, A., Posi, P., Kampala, A., Kaewngao, T., & Chindaprasirt, P. (2021). Beneficial utilization of recycled asphaltic concrete aggregate in high calcium fly ash geopolymer concrete. Case Studies in Construction Materials, 15, 615. doi:10.1016/j.cscm.2021.e00615.

[34] Rukzon, S., & Chindaprasirt, P. (2012). Utilization of bagasse ash in high-strength concrete. Materials & Design, 34, 45–50. doi:10.1016/j.matdes.2011.07.045.

[35] Wongkvanklom, A., Posi, P., Kasemsiri, P., Sata, V., Cao, T., & Chindaprasirt, P. (2021). Strength, thermal conductivity and sound absorption of cellular lightweight high calcium fly ash geopolymer concrete. Engineering and Applied Science Research, 48(4), 487-496.

[36] ASTM C109/C109M-21. (2024). Standard Test Method for Compressive Strength of Hydraulic Cement Mortars (Using 2-in. or [50 mm] Cube Specimens). ASTM International, Pennsylvania, United States. doi:10.1520/C0109_C0109M-21.

[37] ASTM C138/C138M-24a. (2024). Standard Test Method for Density (Unit Weight), Yield, and Air Content (Gravimetric) of Concrete. ASTM International, Pennsylvania, United States. doi:10.1520/C0138_C0138M-24A.